Ultrafast edge photoexcitation and coherent oscillations in tunnel-coupled double quantum wells

F. T. Vasko and O. E. Raichev
Institute of Semiconductor Physics, National Academy of Sciences of the Ukraine, Prospekt Nauki 45, Kiev-28, 252650, Ukraine
(Received 14 November 1994; revised manuscript received 7 February 1995)

Photoexcitation of electrons in double quantum wells is studied as a function of level splitting, duration of the light pulse τ_p, and light frequency. Dynamics of transitions between the upper states of the valence band and the tunnel-coupled pair of conduction-band states is considered in the collisionless approximation. The nonmonotonic temporal dependence of the photoexcited electron concentration (the saturation value of this concentration determines the time-integrated interband photoluminescence intensity) is obtained for the times $t \sim \tau_p$. Transition from the nonperiodic (at $t \sim \tau_p$) to the periodic (at $t \gg \tau_p$) behavior of the dipole moment oscillations is described.

I. INTRODUCTION

Electronic properties of tunnel-coupled double quantum wells (DQW's) are currently studied in various experiments, including time-resolved photoluminescence spectroscopy as a most common and direct method.[1] For a detailed description of such experiments, it is necessary to study optical excitation of DQW's under a subpicosecond laser pulse pumping, and to describe coherent phenomena just after the excitation, when a nearly collisionless regime of electron density evolution is realized. The difference between such coherent phenomena in DQW's and analogous phenomena in bulk,[2,3] superlattice[4] and single quantum well[5] samples is caused by the fact that the pulse duration τ_p can be comparable with the period of coherent oscillation in DQW's, which is equal to $2\pi\hbar/\Delta_T$, where Δ_T is the energy splitting between the DQW's levels. Characteristics of the optical pumping in DQW's (such as amplitude and phase evolution of the electron density matrix) considerably depend on the correlation between these two time constants. For this reason, examination of the coherent optical excitations in DQW's is a subject of interest. Investigation of the coherent phenomena in DQW's has been done in several experiments. The coherent submillimeter-wave emission caused by the interwell dipole moment oscillations has been observed in Ref. 6. The optical pump-probe measurements of phase coherence of such oscillations have been done in Refs. 7, 8. Another pump-probe experiment[9] has revealed coherent oscillations of the light transmission in DQW's.

Theoretical analysis of the coherent photoexcitation in DQW's has been done in a few papers. In Ref. 8, a model of three discrete levels (without longitudinal motion) has been used for the explanation of the pump-probe experiments.[7,8] Recently, some numerical results, which take into account the longitudinal motion of the photoexcited carriers and Coulomb interaction between them have been reported.[10] However, dependence of the photoexcited electrons concentration and DQW's dipole moment on the light frequency and splitting of the tunnel-coupled levels has not been studied in detail.

In this paper, we present an analytical calculation of the density matrix evolution in DQW's under the spatially uniform excitation by the ultrashort laser pulse. We examine optical transition of the electrons from the left quantum well (QW) valence band state to the pair of tunnel-coupled conduction-band states (see Fig. 1). We consider a collisionless approximation, assuming that both pulse duration and coherent oscillations period are small in comparison with the dephasing times caused by different scattering mechanisms. When the optical pumping frequency is close to the interband transitions edge, and the spectral width of the pulse $\hbar/\tau_p$ is smaller than the optical phonon energy, the fast dephasing due

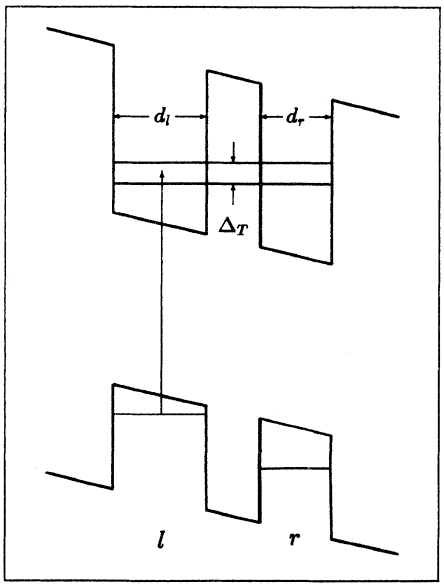

FIG. 1. Band diagram and photoexcitation scheme of the asymmetric double quantum wells.

to the optical phonon emission is not important and the regime of electron density evolution is indeed close to collisionless (such a regime has been observed in the above-mentioned experiments[6–8]). Considering low pumping intensities, we neglect all kinds of nonlinearities, such as the influence of the laser electric field on the electron states, nonlinearities due to saturation phenomena (Moss-Burstein effect), nonlinearities due to Coulomb interaction of carriers, and so on.

We consider the electron density matrix, which slowly varies during the time $2\pi/\omega$ (here ω is the laser light frequency). Evolution of this density matrix is described by a 2×2 matrix quantum kinetic equation containing a non-Markovian generation term. In a collisionless approximation, this equation is transformed to a balance equation for the total electron concentration n_t and to a system of balance equations for the components of the "isospin density vector" $\mathbf{n}_t$. This system is analogous to the Bloch equations in the theory of magnetic moment evolution.[11] A z component of the isospin density vector describes oscillations of the DQW's dipole moment, which is connected with the evolution of the x, y components. On the other hand, temporal evolution of the electron concentration in the left QW determines the intensity of interband photoluminescence.

The paper is organized as follows. In Sec. II, we describe a transformation from the general equations of the Kane's band model for DQW's to the model that takes into account two tunnel-coupled electron levels and a single hole level (Fig. 1). In Sec. III, the balance equations for n_t and $\mathbf{n}_t$ are derived. The solution of these equations in a collisionless approximation is presented in Sec. IV, V, where n_t and $\mathbf{n}_t$ are expressed through the two-time integrals. Subsequent numerical calculation of these integrals is done within a model of the Gaussian-shaped laser pulse, i.e., with the assumption that the pumping intensity is proportional to $\exp[-(t/\tau_p)^2]$. The evolution of the concentration and dipole moment is discussed. Concluding remarks are done in the last section, and the Appendix contains the evaluation of the interband photogeneration rate for the quantum kinetic equation from Sec. III.

II. MODEL OF DOUBLE QUANTUM WELLS

To describe the electron and hole states near the extrema of the conduction and valence bands, we start from the 8×8 Kane's matrix Hamiltonian,

$$\hat{H} = \frac{\mathbf{P}^2}{2m_{\rm hh}} + \hat{\mathbf{v}}\cdot\mathbf{P} + \hat{U}(z)\ , \tag{1}$$

where $\mathbf{P}$ is the three-dimensional electron momentum operator, the diagonal matrix $\hat{U}(z)$ describes variations of the conduction- and valence-band energies along the growth axis OZ, $\hat{\mathbf{v}}$ is the nondiagonal velocity matrix, and $m_{\rm hh}$ is the heavy-hole mass. In the type I heterostructures, when the band offsets at the interfaces are small in comparison with the band-gap energy, one can consider independent equations for the envelope wave functions of the electron and hole states [in a similar way to the single QW (Refs. 12 and 13)]. The spin-degenerate electron states are described by the columnar envelope wave function, where the first and second components (only these components are important near the conduction-band extremum) are determined by the effective-mass Hamiltonian,

$$\frac{\mathbf{P}^2}{2m_c} + U_c(z), \tag{2}$$

where m_c is the electron effective mass and $U_c(z)$ is the conduction-band potential energy. In the following, we restrict ourselves by the consideration of a pair of tunnel-coupled electron states of the DQW's, when the envelope wave functions of Hamiltonian (2) can be represented as a superposition of two orbitals. Such orbitals describe ground states in the left (l) and right (r) QW's and are denoted in following as $|l_c\rangle$, $|r_c\rangle$, respectively. In the basis of l and r orbitals (so-called "isospin" representation), Hamiltonian (2) transforms into 2×2 matrix Hamiltonian,

$$\frac{\mathbf{p}^2}{2m_c} + \varepsilon_c + \frac{\Delta}{2}\hat{\sigma}_z + T\hat{\sigma}_x, \tag{3}$$

where $\mathbf{p}$ is the 2D momentum, Δ is the level splitting (in the absence of tunneling), T is the tunneling matrix element, $\hat{\sigma}_i$ are Pauli matrices, ε_c is the electron energy corresponding to the middle point between the tunnel-coupled levels. Introduction of this Hamiltonian and expressions of Δ and T through the DQW's parameters are given in Refs. 14. The matrix part of the Hamiltonian (3) describes an additional (in comparison with the single QW case) degree of freedom, connected with a possibility of an electron wave packet motion between the wells. According to (3), the spectrum of the tunnel-coupled electron states is given by the expression

$$\varepsilon_c(p) = \varepsilon_c + \frac{p^2}{2m_c} \pm \frac{\Delta_T}{2}\ , \tag{4}$$

where $\Delta_T = \sqrt{\Delta^2 + (2T)^2}$. At $\Delta = 0$ (tunneling resonance), the electron wave functions are symmetrical and asymmetric superpositions of the l and r orbitals. At $\Delta > 0$ ($\Delta < 0$), the upper-energy state ("+") is localized mostly in the l (r) well, while the lower-energy state ("−") is localized mostly in the r (l) well.

Hole states in the valence band of DQW's are described by the Luttinger 4×4 matrix Hamiltonian. Spectrum of the ground hole states in DQW's can be obtained analytically in the approximation of strongly different light- and heavy-hole masses $m_{\rm lh} \ll m_{\rm hh}$, see Ref. 15. In this paper, we consider asymmetric DQW's, where tunneling resonance of the electron states is achieved by application of the transverse electric field (see Fig. 1). In such a field, the hole levels originating from different wells are separated enough in energies, and we need only the l QW hole state to describe edge photoexcitation. Near the valence-band extremum, the spectrum of the two-dimensional ground hole state is given by

$$\varepsilon_h(p) = \varepsilon_h - p^2/2m_h\ , \tag{5}$$

where ε_h is the hole level energy, and m_h is the two-dimensional (2D) hole mass, which is comparable with the light-hole mass under the condition $m_{\rm lh} \ll m_{\rm hh}$ (see Ref. 16). The envelope wave function for this state is expressed through the l QW hole orbital $|l_h)$.

Transitions between the electron and hole states, due to interaction with the laser radiation are described in the dipole approximation by the following perturbation Hamiltonian,

$$\delta\hat{H}_t e^{-i\omega t} + \text{H.c.}\,, \qquad \delta\hat{H}_t = \frac{ie}{\omega}\mathbf{E}\cdot\hat{\mathbf{v}}w(t), \tag{6}$$

where $\mathbf{E}$ is the laser electric field amplitude, and $w(t)$ is the envelope form-factor of this field, which is slowly varying in time compared with the optical frequency ω. This perturbation Hamiltonian is obtained in the usual way from Eq. (1), by a substitution of the kinematic momentum $\mathbf{p} - e\mathbf{A}(\mathbf{t})/c$ [$\mathbf{A}(\mathbf{t})$ is the vector potential], instead of $\mathbf{p}$ and the neglection of the terms proportional to $\mathbf{A}^2/m_{\rm hh}$ and $\mathbf{p}\cdot\mathbf{A}/m_{\rm hh}$, which describe only intraband motion. Probabilities of optical transitions between the ground valence-band state in l QW and a pair of the tunnel-coupled conduction-band states are proportional to the nondiagonal (with respect to the band index) matrix elements of the perturbation Hamiltonian:

$$|(l_c|\mathbf{E}\cdot\hat{\mathbf{v}}|l_h)|^2 = \mathcal{P}^2(l_c|l_h)^2E_\perp^2/2, \tag{7}$$

similarly to the single QW case.[12,13] Here, $\mathcal{P}$ is the interband velocity of the Kane's model, $E_\perp^2 = E_x^2 + E_y^2$. Due to the same parity of the ground-state electron and hole envelope wave functions, the overlap integral of the l−QW orbitals $(l_c|l_h)$ is close to 1 (provided that the transverse electric field is not very strong), and we substitute $(l_c|l_h)$=1 in the following. On the other hand, the interwell overlap integral $(r_c|l_h)$ is exponentially small, due to negligible underbarrier penetration of the orbitals belonging to the different wells, and we neglect $|(r_c|\mathbf{E}\cdot\hat{\mathbf{v}}|l_h)|$.

III. EVALUATION OF THE CONCENTRATION AND ISOSPIN DENSITY BALANCE EQUATIONS

An averaged over the period $2\pi/\omega$ density operator is determined from the quantum kinetic equation,

$$\frac{\partial\hat{\rho}_t}{\partial t} + \frac{i}{\hbar}[\hat{H},\hat{\rho}_t] = \hat{G}_t + \hat{I}_t. \tag{8}$$

Here, $\hat{I}_t$ describes the evolution of the density operator due to the scattering (recombination processes are neglected), and the term $\hat{G}_t$ describes the interband generation of carriers by the laser radiation [see Ref. 17 and Eq. (A4) from the Appendix]:

$$\hat{G}_t = \frac{1}{\hbar^2}\int_{-\infty}^{0} d\tau e^{\lambda\tau - i\omega\tau}\left[\hat{S}_\tau[\delta\hat{H}_{t+\tau},\hat{\rho}_{t+\tau}]\hat{S}_\tau^+, \delta\hat{H}_t^+\right] + \text{H.c.}\,, \tag{9}$$

where $\hat{S}_\tau = \exp[i\hat{H}\tau/\hbar]$. In the following, we apply Eqs. (8), (9) to the three-level model described in the previous section: a single valence-band state in l QW and a pair of tunnel-coupled states in the conduction band. We assume that the laser intensities are small compared with the saturation intensity, and the valence band is fully occupied. In such conditions, the generation term $\hat{G}_t$ should be calculated with $\hat{\rho}_{t+\tau} \simeq \hat{P}_v$, where $\hat{P}_v$ is the valence-band projection operator, which has the single diagonal nonzero matrix element for the valence-band state $(l_h|\hat{P}_v|l_h)$=1.

Projecting Eq. (8) on the conduction-band states and using the momentum representation [Eqs. (3)–(5)], we obtain a 2×2 matrix equation, which describes the behavior of the conduction-band density matrix $\hat{\rho}_{pt}^c$:

$$\frac{\partial\hat{\rho}_{pt}^c}{\partial t} + \frac{i}{\hbar}\left[\frac{\Delta}{2}\hat{\sigma}_z + T\hat{\sigma}_x, \hat{\rho}_{pt}^c\right] = \hat{G}_{pt} + \hat{I}_{pt}^{sc}. \tag{10}$$

Here, $\hat{I}_{pt}^{sc}$ describes the collision-induced relaxation of the conduction electrons, and $\hat{G}_{pt}$ describes electron generation,

$$\hat{G}_{pt} = \frac{1}{2}\left(\frac{e\mathcal{P}E_\perp}{\hbar\omega}\right)^2 w(t)\int_{-\infty}^{0} d\tau \exp[\lambda\tau - i(\Delta\omega - \xi_p)\tau] \times w(t+\tau)\exp\left[\frac{i}{\hbar}\left(\frac{\Delta}{2}\hat{\sigma}_z + T\hat{\sigma}_x\right)\tau\right]\hat{P}_l + \text{H.c.} \tag{11}$$

In this equation $\xi_p = p^2/(2m^*\hbar)$, $m^* = m_c m_h/(m_c + m_h)$ is the reduced mass, $\hat{P}_l = (1+\hat{\sigma}_z)/2$ is the l QW projection operator, and

$$\Delta\omega = \omega - (\varepsilon_c - \varepsilon_h)/\hbar \tag{12}$$

is the difference between the laser frequency and the effective band-gap frequency. Assuming that the pulse duration is small in comparison with the scattering times, we have neglected collision effects in the generation term. The generation term goes to zero at $|t| \gg \tau_p$. Since $\hat{G}_{pt}$ is a nondiagonal matrix, nondiagonal contributions in the density matrix $\hat{\rho}_{pt}^c$ are important for the following calculations.

Below, we consider the evolution of the total electron concentration in the DQW's n_t, as well as the evolution of the "isospin density vector" $\mathbf{n}_t$. These values are defined as

$$n_t = \frac{1}{S}\text{tr}\sum_{\mathbf{p}}\hat{\rho}_{pt}^c, \qquad \mathbf{n}_t = \frac{1}{S}\text{tr}\hat{\vec{\sigma}}\sum_{\mathbf{p}}\hat{\rho}_{pt}^c, \tag{13}$$

where tr denotes trace over the isospin variable and S is the normalization area. Function n_t obeys the equation

$$\frac{\partial n_t}{\partial t} = G_t, \quad G_t = \frac{1}{S}\text{tr}\sum_{\mathbf{p}}\hat{G}_{pt}\,, \tag{14}$$

where the relaxation term has vanished, because the scattering does not change the total number of the electrons. Isospin density vector $\mathbf{n}_t$ obeys the Bloch balance equations,

$$\frac{\partial \mathbf{n}_t}{\partial t} - [\mathbf{L} \times \mathbf{n}_t] = \mathbf{G}_t + \mathbf{I}_t^{sc}, \quad \mathbf{G}_t = \frac{1}{S} \mathrm{tr} \hat{\sigma} \sum_{\mathbf{p}} \hat{G}_{pt} \ , \quad (15)$$

where vector $\mathbf{L} = (2T/\hbar, 0, \Delta/\hbar)$ describes coherent oscillations, and the last term $\mathbf{I}_t^{sc}$ describes dephasing (relaxation of the isospin density). When both the excitation time τ_p and the coherent oscillation period $2\pi\hbar/\Delta_T$ are small in comparison with the relaxation time, we can neglect the relaxation term $\mathbf{I}_t^{sc}$ in the description of the electron density evolution during the excitation and just after it. Equations (14) and (15) must be solved with the initial conditions $n_t = 0$ and $\mathbf{n}_t = 0$ at $t = -\infty$.

IV. TIME EVOLUTION OF THE ELECTRON DENSITY

After substitution of the expression (11) in the right-hand part of Eq. (14) and trace calculation, we obtain the following expression for the generation rate:

$$G_t = \frac{1}{2} \left(\frac{e\mathcal{P}E_\perp}{\hbar\omega} \right)^2 w(t) \int_{-\infty}^{0} d\tau w(t+\tau) \frac{1}{S} \sum_{\mathbf{p}} \times [(1+\eta)\cos(\Delta\omega - \xi_p - \omega_T/2)\tau + (1-\eta)\cos(\Delta\omega - \xi_p + \omega_T/2)\tau], \quad (16)$$

where $\omega_T = \Delta_T/\hbar$ is the coherent oscillations frequency, and $\eta = \Delta/\Delta_T$ determines the interwell coupling strength. The solution of Eq. (14) is obtained in a straightforward way, after integration of G_t over time:

$$n_t = \frac{N}{\pi\tau_p} \int_{-\infty}^{t} d\tau' w(\tau') \int_{-\infty}^{0} d\tau w(\tau'+\tau) \int_0^\infty d\xi \times [(1+\eta)\cos(\Delta\omega - \xi - \omega_T/2)\tau + (1-\eta)\cos(\Delta\omega - \xi + \omega_T/2)\tau], \quad (17)$$

where characteristic concentration N is defined by

$$N = \frac{m^*}{4\hbar} \left(\frac{e\mathcal{P}E_\perp}{\hbar\omega} \right)^2 \tau_p \ , \quad (18)$$

and the sums over the 2D momentum $\mathbf{p}$ are transformed into simple integrals over $\xi = \xi_p$. Such integrals are evaluated with the use of the well-known relation

$$\int_0^\infty d\xi \exp[i(t+i0)\xi] = \pi\delta(t) + i\mathrm{P}(1/t), \quad (19)$$

where $+i0$ in the exponent appears due to damping and P means the principal value. We have

$$n_t = N \int_{-\infty}^{t} \frac{d\tau'}{\tau_p} \left\{ w^2(\tau') + \int_{-\infty}^{0} \frac{d\tau}{\pi\tau} w(\tau') w(\tau'+\tau) [(1+\eta)\sin(\Delta\omega - \omega_T/2)\tau + (1-\eta)\sin(\Delta\omega + \omega_T/2)\tau] \right\}. \quad (20)$$

Figure 2(a,b) represents the evolution of the electron concentration calculated from Eq. (20), with $w(t) = \exp[-(t/\tau_p)^2]$ at different values of light frequency and different correlations between the pulse duration τ_p and coherent oscillations frequency ω_T. Only the resonant case $\Delta = 0$ is shown here. For the excitation below the conduction-band edge ($\Delta\omega < -\omega_T/2$), evolution of the concentration is nonmonotonic, with a peak in the region $t \sim \tau_p$. The peak is more prominent for longer pulses [see (b)] Evolution of the electron concentration in the nonresonant case $\Delta \neq 0$ for $\tau_p\omega_T/2\pi = 0.5$ is shown in Fig. 3(a,b). It is seen that for the positive Δ nonmonotonic behavior of n_t can exist also for the excitation above the conduction-band edge. It is connected with the asymmetrical contributions of the l and r orbitals in the electron states: at $\Delta > 0$, the lowest electron state is localized mostly in the right well, while the excitation at $t \sim \tau_p$ occurs in the left well.

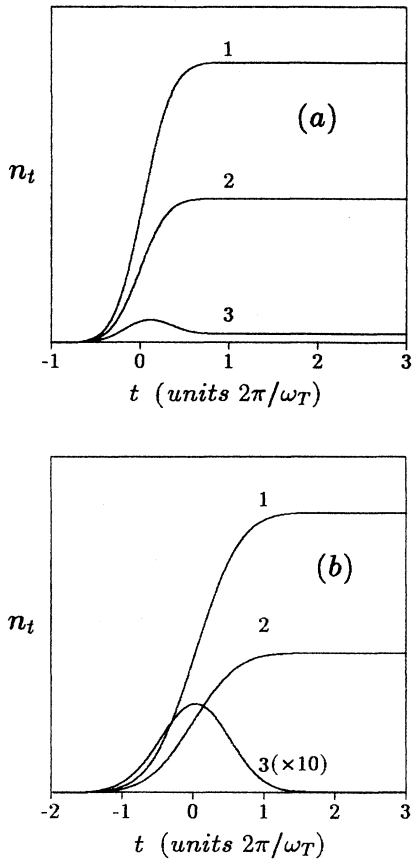

FIG. 2. Time evolution of the conduction electrons concentration (arbitrary units), for $\tau_p\omega_T/2\pi = 0.5$ (a) and $\tau_p\omega_T/2\pi = 1.0$ (b), at $\Delta\omega = \omega_T$ (1), $\Delta\omega = 0$ (2), and $\Delta\omega = -\omega_T$ (3).

At $t \gg \tau_p$ the electron concentration is saturated. The saturation value can be expressed through the error function according to the following equation:

$$n_{+\infty} = \sqrt{\frac{\pi}{2}} N \left\{ 1 + \frac{1+\eta}{2} \mathrm{erf}\left[(\Delta\omega - \omega_T/2)\tau_p/\sqrt{2} \right] + \frac{1-\eta}{2} \mathrm{erf}\left[(\Delta\omega + \omega_T/2)\tau_p/\sqrt{2} \right] \right\}. \quad (21)$$

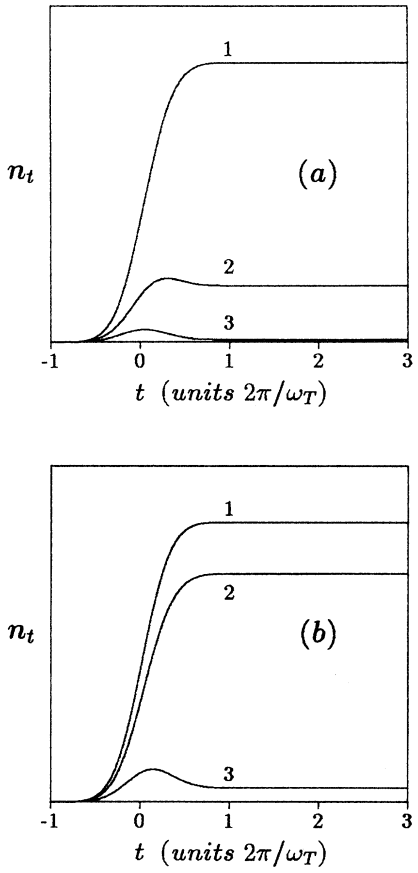

FIG. 3. The same as in Fig. 2(a) for nonzero splitting Δ: Δ/Δ_T =0.7 (a) and $\Delta/\Delta_T = -0.7$ (b).

At $\Delta\omega\tau_p \ll -1$, $n_{+\infty}$ goes to zero (no absorption). At $\Delta\omega\tau_p \gg 1$, $n_{+\infty}$ does not depend on $\Delta\omega$ and ω_T. In the latter case, N is connected with the total concentration of the photoexcited electrons by the simple relation $n_{+\infty} = \sqrt{2\pi}N$. Typical electron concentrations generated in the experiments[6–8] are below 10^{10} cm^{-2}, which approximately corresponds to the single-pulse intensities below 3 erg cm^{-2}.

V. OSCILLATIONS OF THE DIPOLE MOMENT

In the collisionless approximation, we neglect the relaxation term $\mathbf{I}_t^{sc}$ in the right-hand part of the system (15). The remaining contribution in the right-hand part arises from the generation term, which is a three-component vector $\mathbf{G}_t = (G_x, G_y, G_z)$ with

$$G_x = \frac{T}{\Delta_T}\left(\frac{e\mathcal{P}E_\perp}{\hbar\omega}\right)^2 w(t)\int_{-\infty}^{0} d\tau w(t+\tau)\frac{1}{S}\sum_{\mathbf{p}} \times[\cos(\Delta\omega - \xi_p - \omega_T/2)\tau - \cos(\Delta\omega - \xi_p + \omega_T/2)\tau], \quad (22)$$

$$G_y = -\frac{T}{\Delta_T}\left(\frac{e\mathcal{P}E_\perp}{\hbar\omega}\right)^2 w(t)\int_{-\infty}^{0} d\tau w(t+\tau)\frac{1}{S}\sum_{\mathbf{p}} \times[\sin(\Delta\omega - \xi_p - \omega_T/2)\tau - \sin(\Delta\omega - \xi_p + \omega_T/2)\tau], \quad (23)$$

and $G_z = G_t$ [see Eq. (16)]. Solution of the system (15) can be easily found after Fourier transformation in time, which transforms (15) into a system of three linear equation. After determination of the Fourier components of the isospin density, we perform an inverse Fourier transformation and obtain $\mathbf{n}_t$. It is convenient to write components n_x, n_y, n_z of $\mathbf{n}_t$ in the following way:

$$n_x(t) = N\frac{2T}{\Delta_T}\left[\Phi_0(t) - \frac{\Delta}{\Delta_T}\Phi_1(t)\right], \quad (24)$$

$$n_y(t) = N\frac{2T}{\Delta_T}\Phi_2(t), \quad (25)$$

$$n_z(t) = N\left[\frac{\Delta}{\Delta_T}\Phi_0(t) + \frac{4T^2}{\Delta_T^2}\Phi_1(t)\right], \quad (26)$$

where

$$\Phi_0(t) = \int_{-\infty}^{t}\frac{d\tau'}{\tau_p}\left\{\eta w^2(\tau') + \int_{-\infty}^{0}\frac{d\tau}{\pi\tau}w(\tau')w(\tau'+\tau) \times[(1+\eta)\sin(\Delta\omega - \omega_T/2)\tau - (1-\eta)\sin(\Delta\omega + \omega_T/2)\tau]\right\}, \quad (27)$$

$$\begin{pmatrix}\Phi_1(t)\\ \Phi_2(t)\end{pmatrix} = \int_{-\infty}^{t}\frac{d\tau'}{\tau_p}\left\{w^2(\tau')\begin{pmatrix}\cos\omega_T(\tau'-t)\\ \sin\omega_T(\tau'-t)\end{pmatrix} + \int_{-\infty}^{0}\frac{d\tau}{\pi\tau}w(\tau')w(\tau'+\tau)2\sin(\Delta\omega\tau) \times\begin{pmatrix}\cos\omega_T(\tau/2+\tau'-t)\\ \sin\omega_T(\tau/2+\tau'-t)\end{pmatrix}\right\}. \quad (28)$$

Functions $\Phi_1(t)$ and $\Phi_2(t)$ describe the oscillating contribution in the isospin density evolution, while $\Phi_0(t)$ describes the nonoscillating contribution. Equations (24)–(28) show that all components of the isospin density oscillate with time. It is important to consider the component $n_z(t)$, because it is connected with the potential $\Delta\varphi$ caused by the dipole moment of DQW's:

$$\Delta\varphi \sim e\Delta z n_z(t), \quad (29)$$

where Δz is the separation between the l and r orbitals (this value is close to the distance between the centers of the quantum wells).

Figure 4(a–c) and Fig. 5(a,b) illustrate behavior of the dipole moment at $\Delta = 0$ and $\Delta \neq 0$, respectively. A complex evolution of the dipole moment at $t \sim \tau_p$ takes place when τ_p is comparable with $2\pi/\omega_T$. At $t \gg \tau_p$, the dipole moment has periodic behavior, which is described by the equation

$$n_z(t) = N\sqrt{\frac{\pi}{2}}\eta\left\{\eta + \frac{1+\eta}{2}\mathrm{erf}\left[(\Delta\omega - \omega_T/2)\tau_p/\sqrt{2}\right]\right.$$
$$\left. - \frac{1-\eta}{2}\mathrm{erf}\left[(\Delta\omega + \omega_T/2)\tau_p/\sqrt{2}\right]\right\}$$
$$+N\sqrt{\frac{\pi}{2}}\frac{4T^2}{\Delta_T^2}\left[1 + \mathrm{erf}(\Delta\omega\tau_p/\sqrt{2})\right]\cos\omega_T t. \tag{30}$$

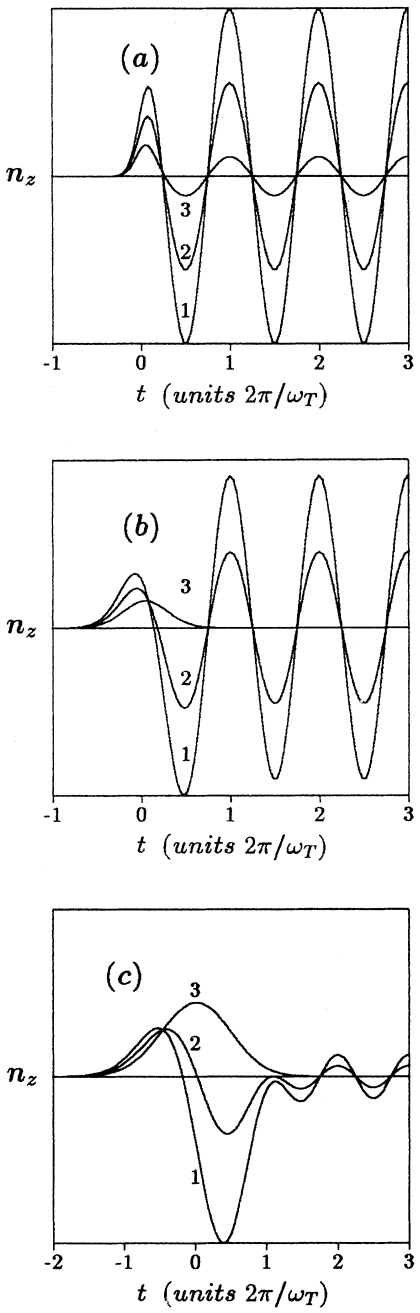

FIG. 4. Time evolution of the dipole moment of DQW's (arbitrary units), for $\tau_p\omega_T/2\pi = 0.2$ (a), $\tau_p\omega_T/2\pi = 0.5$ (b), and $\tau_p\omega_T/2\pi = 1.0$ (c); labels 1, 2, 3 have the same meaning as in Fig. 2.

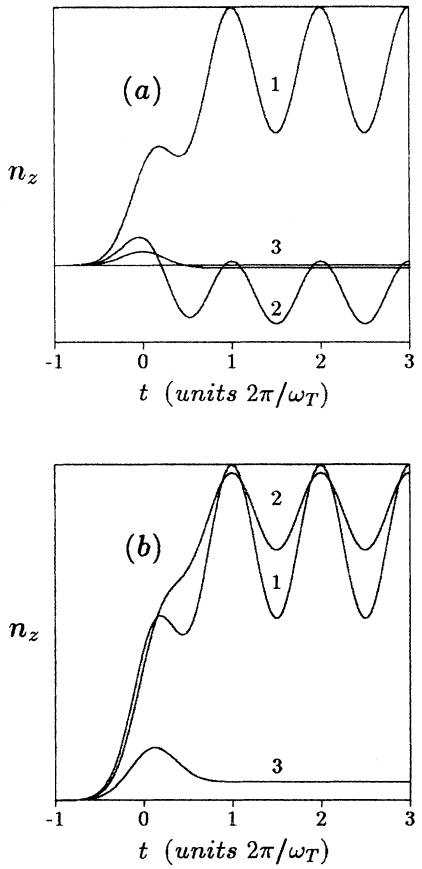

FIG. 5. The same as in Fig. 4(b) for nonzero splitting Δ: $\Delta/\Delta_T = 0.7$ (a) and $\Delta/\Delta_T = -0.7$ (b).

The periodic contribution is described by the last part of this equation. We stress that the amplitude of this contribution depends on the correlation between the pulse duration and photon frequency, but the phase is independent on this correlation. The value of the phase is the same for arbitrary pulse shape, provided that the pulse is symmetrical. In addition, the nonperiodic contribution in the dipole moment exists at $\Delta \neq 0$, as it is also seen from Fig. 5. Such a contribution is sensitive to the sign of Δ.

In the existing experiments,[6–8] rather short pulses (τ_p =80–160 fs) have been applied, that corresponds to $\tau_p\omega_T/2\pi \simeq 0.2$ [calculated dipole moment oscillations for this case are illustrated in Fig. 3(a)]. In this situation, an approximation of the pulse shape by the δ function can be used. The oscillating part of the dipole moment in this approximation is proportional to

$$\int_{-\infty}^{t} d\tau w^2(\tau)\cos\omega_T(t-\tau), \tag{31}$$

and it is independent on the laser frequency, which is not surprising, because very short pulses are spectrally broad and since $\Delta\omega\tau_p \ll 1$, there must be no dependence of all observable values on $\Delta\omega$.

VI. CONCLUSIONS

In this paper, we have investigated the edge photoexcitation of carriers in the DQW's by the ultrafast laser pulses. A laser pulse at $t = 0$ generates an electronic wave packet in one of the wells. This packet oscillates between the wells with the period $2\pi\hbar/\Delta_T$ determined by the level splitting of the DQW's. As a result, the DQW structure manifests itself as a dipole oscillator emitting terahertz radiation. When the laser pulse duration τ_p is comparable with the coherent oscillations period, it is necessary to take into account the movement of the electron wave packet during the excitation time. In such conditions, time evolution of the DQW's dipole moment has complex behavior in the time interval $t \sim \tau_p$. Nevertheless, asymptotic behavior of the dipole moment at $t \gg \tau_p$ is periodic and is characterized by a constant phase, which is independent on characteristics of the structure and photoexcitation, provided that the excitation pulse is symmetrical.

On the other hand, not only the distribution of electrons between QW's, but also the total concentration n_t of photoexcited electrons show complex behavior under ultrashort pulse pumping. The dependence of the saturation value $n_{+\infty}$ of this concentration from $\Delta\omega$ and Δ can be measured by the time-integrated photoluminescence. By means of the time-resolved photoluminescence,[1] one can measure time evolution of the l QW concentration, which is equal to the combination $n_t + n_z(t)$.

In order to describe these phenomena, we evaluated the matrix quantum kinetic equation for electrons in DQW's. Such an equation contains a nondiagonal term, which describes the generation of the electrons by the light pulse. We took into account longitudinal motion of electrons and obtained the analytical expressions for the concentration of photoexcited electrons and the DQW's dipole moment in the case of finite pulse duration. Such expressions allowed us to investigate the time evolution of the concentration and dipole moment for different photon energies, pulse durations, and DQW's parameters. In our calculations, we have neglected the scattering of electrons, which is not important for the generality of our results in the case when both the pulse duration and coherent oscillations periods are small in comparison with the relaxation times. (We stress here that in the existing calculations,[8,10] the scattering is taken into account phenomenologically, which does not permit us to estimate the dephasing times properly.) The next approximation is that we have neglected the Coulomb interaction between the electrons and holes, which gives rise to excitonic effects.

The calculated time evolution of the DQW's dipole moment is consistent with the existing experiments,[6,7] where the excitation pulse duration has been small in comparison with the coherent oscillations period. In the case when the pulse duration is comparable with the coherent oscillations period, our calculations show a more complex behavior of the dipole moment during the excitation. To reveal such peculiarities, further experimental studies are necessary.

ACKNOWLEDGMENT

This work has been supported by the International Science Foundation, Grant No. U65000.

APPENDIX

Here, we evaluate the generation rate for Eq. (8), starting from the general equation for the density operator $\hat{R}_t$:

$$\frac{\partial \hat{R}_t}{\partial t} + \frac{i}{\hbar}[\hat{H}, \hat{R}_t] = \frac{1}{i\hbar}[\delta\hat{H}_t e^{-i\omega t} + \text{H.c.}, \hat{R}_t]. \quad \text{(A1)}$$

Using the initial condition $\hat{R}_{t\to-\infty} = \hat{R}_0$, ($[\hat{H}, \hat{R}_0] = 0$), we can rewrite this equation as

$$\hat{R}_t = \hat{R}_0 + \frac{1}{i\hbar}\int_{-\infty}^{t} d\tau e^{\lambda\tau}\hat{S}_{\tau-t}[\delta\hat{H}_\tau e^{-i\omega\tau} + \text{H.c.}, \hat{R}_\tau]\hat{S}^+_{\tau-t}, \quad \text{(A2)}$$

($\hat{S}_t$ is introduced in Sec. III). Substituting (A2) into the right-hand part of (A1) and replacing τ by $\tau + t$, we obtain in this part,

$$\frac{1}{i\hbar}[\delta\hat{H}_t e^{-i\omega t} + \text{H.c.}, \hat{R}_0] - \frac{1}{\hbar^2}\int_{-\infty}^{0} d\tau e^{\lambda\tau}[(\delta\hat{H}_t e^{-i\omega t} + \text{H.c.}), \times\hat{S}_\tau[(\delta\hat{H}_{t+\tau}e^{-i\omega(t+\tau)} + \text{H.c.}), \hat{R}_{t+\tau}]\hat{S}^+_\tau]. \quad \text{(A3)}$$

In this paper, we consider the case of high frequency pumping ($1/\omega$ is small in comparison with all typical times of the problem) and are interesting in the slowly changing part $\hat{\rho}_t$ of the density operator. Neglecting the contributions in (A3), which are proportional to $\exp(\pm ik\omega t)$ ($k = 1, 2, \ldots$), we obtain an averaged over the period $2\pi/\omega$ quantum kinetic equation,

$$\frac{\partial\hat{\rho}_t}{\partial t} + \frac{i}{\hbar}[\hat{H}, \hat{\rho}_t] = \frac{1}{\hbar^2}\int_{-\infty}^{0} d\tau e^{\lambda\tau} \times(e^{-i\omega\tau}[\hat{S}_\tau[\delta\hat{H}_{t+\tau}, \hat{\rho}_{t+\tau}]\hat{S}^+_\tau, \delta\hat{H}^+_t] + \text{H.c.}). \quad \text{(A4)}$$

The right-hand part of (A4) transforms to Eq. (9) (the collision integral $\hat{I}_t$ can be evaluated in the usual way).

[1] Ph. Roussignol, A. Vinatierri, L. Carraresi, M. Colocci, and A. Fasolino, Phys. Rev. B **44**, 8873 (1991).
[2] X.-C. Zhang, B. B. Xu, J. T. Darrow, and D. H. Auston, Appl. Phys. Lett. **56**, 1101 (1990); B. B. Xu, X.-C. Zhang, and D. H. Auston, Phys. Rev. Lett. **67**, 2709 (1991).
[3] A. V. Kuznetsov and C. J. Stanton, Phys. Rev. B **48**, 10 828 (1993); F. Rossi, S. Haas, and T. Kuhn, Semicond. Sci. Technol. **9**, 411 (1994); F. J. Adler, P. Kocevar, J. Schilp, T. Kuhn, and F. Rossi, *ibid.* **9**, 446 (1994).
[4] L. Xu, X.-C. Zhang, D. H. Auston, and W. I. Wang, Appl. Phys. Lett. **59**, 3562 (1991).
[5] P. C. M. Planken, I. Brenner, M. C. Nuss, M. S. C. Luo, S. L. Chuang, and L. N. Pfeiffer, Phys. Rev. B **49**, 4668 (1994).
[6] H. G. Roskos, M. C. Nuss, J. Shah, K. Leo, D. A. B. Miller, A. M. Fox, S. Schmitt-Rink, and K. Köhler, Phys. Rev. Lett. **68**, 2216 (1992).
[7] P. C. M. Planken, I. Brenner, M. C. Nuss, M. S. C. Luo, and S. L. Chuang, Phys. Rev. B **48**, 4903 (1993).
[8] M. S. C. Luo, S. L. Chuang, P. C. M. Planken, I. Brenner, and M. C. Nuss, Phys. Rev. B **48**, 11 043 (1993).
[9] K. Leo, J. Shah, E. O. Göbel, J. P. Gordon, and S. Schmitt-Rink, Semicond. Sci. Technol. **7**, B394 (1992).
[10] T. Kuhn, E. Binder, and G. Mahler (unpublished).
[11] R. W. White, *Quantum Theory of Magnetism* (Springer-Verlag, Berlin, 1983).
[12] O. E. Raichev and F. T. Vasko, Phys. Rev. B **50**, 5462 (1994).
[13] F. T. Vasko, *Electron States and Optical Transitions in Semiconductor Heterostructures* (Naukova Dumka, Kiev, 1993).
[14] A. Yariv, S. Lindsey, and U. Sivan, J. Appl. Phys. **58**, 3669 (1985); F. T. Vasko, O. G. Balev, and P. Vasilopoulos, Phys. Rev. B **47**, 16 433 (1993).
[15] F. T. Vasko and O. E. Raichev, Zh. Eksp. Teor. Fiz. **104,** 3103 (1993) [Sov. Phys. JETP **77**, 452 (1993)].
[16] M. I. Dyakonov and A. V. Khaetski, Zh. Eksp. Teor. Fiz. **82**, 1584 (1982) [Sov. Phys. JETP **55**, 917 (1982)].
[17] F. T. Vasko, Fiz. Tekh. Poluprovodn. **19**, 1319 (1985) [Sov. Phys. Semicond. **19**, 808 (1985)].